ACS Catalysis

Research Article

pubs.acs.org/acscatalysis

Molybdenum-Based Polyoxometalates as Highly Active and Selective Catalysts for the Epimerization of Aldoses

Feifei Ju,[†] David VanderVelde,[‡] and Eranda Nikolla*,[†]

[†]Department of Chemical Engineering and Material Science, Wayne State University, Detroit, Michigan 48202, United States

[‡]Division of Chemistry and Chemical Engineering, California Institute of Technology, Pasadena, California 91125, United States

Supporting Information

ABSTRACT: In this contribution, we report on the high activity and selectivity of Keggin structure molybdenum-based polyoxometalates (POMs) in catalyzing the epimerization of aldoses. Near-equilibrium conversions and selectivities were obtained within the first hour of operation under aqueous conditions at relatively low temperatures and a wide range of pHs. Characterization of the molybdenum-based POM catalysts using X-ray diffraction and FTIR studies before and after the reaction showed no evidence of their decomposition. Our studies suggest that the active sites for the reaction are the molybdenum oxide octahedra on the surface of the Keggin structure of the molybdenum-based POMs ($H_3PMo_{12}O_{40}$, $Ag_3PMo_{12}O_{40}$, $Sn_{0.75}PMo_{12}O_{40}$). Further characterization of the system using ^{31}P NMR and X-ray photoelectron spectroscopy experiments showed that the interaction between the aldose (e.g., glucose) and the molybdenum oxide octahedra in the POM results in electron transfer from the aldose to molybdenum, leading to the formation of the reduced form of the POM (also known as heteropoly blue). Isotope labeling experiments demonstrated that the epimerization of glucose using molybdenum-based POMs proceeds via an intramolecular C1−C2 shift mechanism with an activation barrier of as low as ∼96 kJ/mol, obtained using controlled kinetic experiments. These findings open up avenues for the implementation of molybdenum-based POMs as single, selective, and stable catalytic systems for the efficient epimerization of aldoses under aqueous conditions at relatively low temperatures and a wide range of pHs.

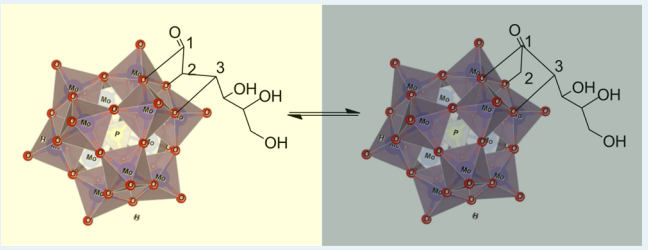

KEYWORDS: *polyoxometalates, aldose epimerization, kinetic isotope effect, Keggin structure, intramolecular carbon shift, heteropoly blue*

1. INTRODUCTION

An important carbohydrate transformation is the epimerization reaction, which involves the transformation of a carbohydrate to its chiral counterpart, the epimer. Scheme 1 shows a schematic of the epimerization of glucose to its epimer, mannose. It has been reported that the theoretical (based on thermodynamic data) equilibrium molar ratio of glucose to mannose in the epimerization reaction is approximately 69.7 to 30.3.[1]

Scheme 1. Schematic of the Epimerization of D-Glucose to D-Mannose

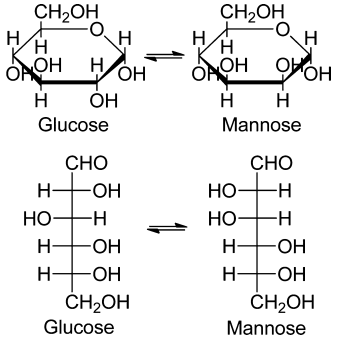

Epimerization is widely used for a number of processes, including the production of rare sugars from more common ones and the production of pharmaceuticals.[2−4] For example, sugars such as D-allose and D-tagatose, which can be epimerized by their corresponding epimers, are used as immunosuppressant[5] and antidiabetic[6] drugs, respectively. The epimerization process is also used in the synthesis of isotope agents. For example, epimerization is employed to synthesize ^{14}C-labeled saccharides from α-[U-^{14}C]glucan.[7]

Epimerization of carbohydrates is catalyzed by enzymes known as epimerases, which are highly selective at epimerizing carbohydrates at different carbon positions.[8] Although they are highly selective, epimerases are very sensitive to operating conditions and can only function over a small range of temperatures and pH values, dramatically restricting their use.[8] In addition, epimerases are difficult to extract and recycle from the reaction medium.[9,10] Therefore, the development of inorganic catalysts for this process is highly desired since they

Received: December 29, 2013
Revised: March 3, 2014
Published: March 25, 2014

can be tuned to operate under various conditions and overcome some of the challenges with the enzymatic systems. The classical method for the epimerization of aldoses using inorganic basic catalysts is the Lobry de Bruyn−Alberda van Ekenstein (LdB−AvE) transformation, which has been studied for many years.[11] One of the main disadvantages of this process is that the basic environment required to catalyze the epimerization causes a series of secondary, undesired reactions along the carbohydrate chain, leading to the formation of many side products such as ketoses and lowering the selectivity toward the desired epimer.[12] For example, the epimerization of glucose using sodium hydroxide has been shown to result in the formation of more than 50 undesired compounds.[13] Aldoses can be epimerized at C2 without the formation of ketoses through other methods, of which the most studied one is the Bilik reaction. In 1970s, Bilik discovered that molybdates under acidic conditions can epimerize aldoses to a thermodynamic equilibrium of the two epimers within 3 h at 90 °C without the formation of the complementary 2-ketose.[14−16] However, in order for molybdate to catalyze aldose epimerization, suitable pH ranges are required for the formation of the active site, which is composed of dinuclear complexes of the molybdate.[14] Ni^{2+} complexes coordinated with ethylenediamine can also epimerize aldoses into their corresponding epimers (glucose to mannose) at a molar ratio of 45:55 in methanol, as reported by Yoshikawa and co-workers.[17−19] One of the challenges with this approach is that the catalytic system is fairly complex, involving interplay among many parameters such as the structure of the nickel complex, the diamine ligand, the configuration of the sugars, and the chirality of the diamine ligand.[20−22] Recent reports have shown that heterogeneous catalysts, such as zeolites with Lewis acid centers, can also be used as catalysts for the epimerization of aldoses in methanol and water. Bermejo-Deval et al.[23] showed that Sn-Beta is highly active toward the epimerization of glucose in methanol, but this system is significantly limited by the low solubility of sugars in methanol. On the other hand, Gunther et al. showed that Sn-Beta can catalyze the epimerization of glucose in water at a glucose to mannose molar ratio of 84:15 within 60 min at 85 °C if coupled with sodium borate, which coordinates with the Sn site in the zeolite to catalyze the reaction.[24]

Here, for the first time, we report the use of a single catalyst, a molybdenum-based polyoxometalate (POM), for the epimerization of aldoses with high activity and selectivity under aqueous conditions. Most of the inorganic catalysts discussed above require either the addition of a Brønsted acid or coordination with ethylenediamine or sodium borate to achieve high conversions and selectivities for the epimerization of aldoses under aqueous conditions. POMs are discrete anionic metal−oxygen clusters that are built from the assembly of $\{MO_x\}$ polyhedrons, where M is usually V^{IV}, V^{V}, Mo^{VI}, or W^{VI}.[25] POMs have been extensively studied for many years and are mainly used as acid and oxidative catalysts because of their strong Brønsted acidities and oxidation potentials.[26−36] One of the most studied and stable POM structures is the Keggin structure, with a formula that is generally described as $H_{8-x}XM_{12}O_{40}^{x-8}$, where X is the central atom, M is the metal ion, and x is the oxidation state of the metal ion.[37] Although POMs have found wide use in oxidative catalysis, they have never been used for the epimerization of molecules such as aldoses under aqueous conditions.[38,39] Herein we report that Keggin structure molybdenum-based POMs catalyze the epimerization of aldoses under aqueous conditions, resulting in near-equilibrium conversions with high selectivity within 60 min of operation. No decomposition of the Keggin anion, $PMo_{12}O_{40}^{3-}$, was detected after the reaction, as corroborated by X-ray diffraction (XRD) and Fourier transform IR (FTIR) spectroscopy. ^{31}P NMR and X-ray photoelectron spectroscopy (XPS) studies indicated that during the epimerization process electron transfer between the aldose and POM occurs, leading to the formation of the reduced form of the POM (also known as heteropoly blue). Furthermore, our isotopic labeling experiments in combination with ^{13}C NMR studies showed that epimerization of glucose using Keggin structure molybdenum-based POMs involves a C1−C2 intramolecular carbon shift with an apparent activation barrier that is much lower (by ∼30 kJ/mol) than those for molybdate catalysts under acidic conditions.

2. EXPERIMENTAL METHODS

2.1. Synthesis of $Ag_3PMo_{12}O_{40}$ and $Sn_{0.75}PMo_{12}O_{40}$. $Ag_3PMo_{12}O_{40}$ and $Sn_{0.75}PMo_{12}O_{40}$ were synthesized using previously reported procedures.[40] Each metal salt of $H_3PMo_{12}O_{40}$ was synthesized from a 0.5 M aqueous solution of $H_3PMo_{12}O_{40}$ via dropwise addition of a stoichiometric quantity of a 0.1 M aqueous solution of silver nitrate or tin(IV) chloride. The mixture was stirred for 1 day at room temperature, followed by centrifugation and drying at 60 °C. $H_3PMo_{12}O_{40}$ was purchased from Sigma-Aldrich and dried at 200 °C for about 20 h before use. The compositions of the Ag-POM and Sn-POM catalysts were confirmed by inductively coupled plasma optical emission spectrometry (ICP-OES) using a HORIBA Jobin Yvon Ultima ICP-OES instrument. The nebulizer was operated at a flow rate of 12 L/min, and samples were run at 1200 W. Standard solutions of silver, tin, and molybdenum were purchased from High Purity Standards. Samples were run against an external calibration curve. The ratios of Ag and Sn to Keggin anion ($PMo_{12}O_{40}^{3-}$) were equal to 3.02 ± 0.01 and 0.76 ± 0.01, respectively, for all of the experiments reported herein.

2.2. Characterization. For ^{13}C NMR spectroscopy, D_2O was used as the solvent for the catalytic reaction. To obtain reasonable signals from the ^{31}P NMR spectra, the molar ratio of Mo (in the catalyst) to glucose was increased to 2.2:1 (the concentration of POM in the solution was 1 M). $^{13}C\{^1H\}$ and $^{31}P\{^1H\}$ NMR spectra were taken on a Varian 400MR instrument (399.8 MHz for ^1H, 100.54 MHz for ^{13}C, and 161.85 MHz for ^{31}P), while $^{31}P\{^1H\}$ diffusion-ordered spectroscopy (DOSY) NMR spectra were taken on a Varian Inova 500 instrument (499.85 MHz for ^1H and 202.34 MHz for ^{31}P). All of the experiments were conducted with standard pulse sequences and parameters using the VnmrJ 3.2 software. For ^{13}C spectra, an acquisition time of 1.31 s and a d1 delay of 1 s were used; for ^{31}P spectra, the acquisition time was 0.8 s and d1 was 1 s. The diffusion experiment was performed with a gradient-compensated stimulated echo sequence using the standard Varian pulse sequence DgcsteSL.

The XPS experiments were conducted using a Kratos Axis Ultra XPS spectrometer with a 150 W Al (Mono) X-ray gun. The instrument was calibrated with respect to Au $4f_{7/2}$ at 83.95 eV. The instrument base pressure was 3×10^{-9} Torr. A 1 M aqueous solution of $AgNO_3$ or $SnCl_4$ was used to precipitate the Keggin anion from solutions with and without glucose, forming $Ag_3PMo_{12}O_{40}$ or $Sn_{0.75}PMo_{12}O_{40}$, respectively. The solid precipitate was dried under vacuum overnight before analysis. Indium foil was used to support the samples in the

dx.doi.org/10.1021/cs401253z | ACS Catal. 2014, 4, 1358−1364

Table 1. Catalytic Performance of Different Polyoxometalates and Their Salts for Aldose Epimerization[a]

entry	catalyst	sugar	T (°C)	t (min)	conversion (%)	selectivity (%)[b]	pH before reaction
1	$H_3PMo_{12}O_{40}$	glucose[c]	80	60	26.2 ± 1.1	91	1.1[e]
2	$H_3PMo_{12}O_{40}$	glucose	80	60	25.5 ± 0.9	94	2.4
3	$H_3PMo_{12}O_{40}$	glucose	80	60	25.0 ± 0.8	93	4.5[e]
4	$H_3PMo_{12}O_{40}$	glucose	100	60	31.3 ± 1.1	90	2.4
5	$Ag_3PMo_{12}O_{40}$	glucose	80	60	26.0 ± 0.8	96	2.9[f]
6	$Sn_{0.75}PMo_{12}O_4$	glucose	80	60	26.1 ± 0.7	95	2.6
7	$H_3PMo_{12}O_{40}$	mannose	80	60	37.8 ± 1.0	93	2.4
8	$H_3PMo_{12}O_{40}$	mannose	100	60	72.9 ± 0.8	91	2.4
9	$H_3PMo_{12}O_{40}$	xylose[c]	80	60	27.0 ± 0.9	93	2.4
10	$H_3PW_{12}O_{40}$	glucose	80	60	0.6 ± 0.2	0	2.4
11	$Ag_3PMo_{12}O_{40}$ (1st recycle)[d]	glucose	80	60	25.2 ± 0.6	95	2.9[f]
12	$Ag_3PMo_{12}O_{40}$ (2nd recycle)[d]	glucose	80	60	24.3 ± 0.9	91	2.9[f]
13	$Ag_3PMo_{12}O_{40}$ (3rd recycle)[d]	glucose	80	60	24.8 ± 1.0	92	2.9[f]

[a]Reaction conditions: 1 g of 10% (w/w) aldose aqueous solution; Mo (or W) to glucose molar ratio = 1:50. [b]Selectivity is reported for the corresponding epimer of the aldose (mannose selectivity in the case of glucose and lyxose selectivity in the case of xylose). All of the conversions and selectivities are averages of three runs. [c]Theoretical equilibrium molar ratios of the two epimers:[41] glucose:mannose = 69.7:30.3; xylose:lyxose = 66.7:33.3. [d]In the recycle experiments, $PMo_{12}O_{40}^{3-}$ was precipitated from solution using $AgNO_3$ to form $Ag_3PMo_{12}O_{40}$, which was dried and reused as the catalyst for the next recycle experiment. The recycle experiment was repeated three times, and the runs are labeled as 1st recycle, 2nd recycle, and 3rd recycle. [e]The solution pH was adjusted using concentrated HCl or NH_4OH. [f]The pH was obtained at 80 °C after heating for 60 min in the absence of glucose in order to obtain a homogeneous mixture of the catalyst in water.

analysis chamber. Powder XRD patterns of the samples were collected using a Rigaku SmartLab diffractometer and Cu Kα irradiation. Attenuated total reflectance (ATR) FTIR measurements were performed on a Nicolet 6700 spectrometer equipped with a MCT-B detector and an ATR stage with a single-reflection diamond crystal.

2.3. Catalytic Reactions. All of the reactions with aldoses were conducted in 5 mL thick-walled glass batch reactors (VWR) containing a small magnetic stirring bar. Typically, in a reaction with D-glucose (Sigma-Aldrich, ≥99%), catalyst was added at a 1:50 metal/glucose molar ratio to a 10% (w/w) glucose aqueous solution. After the catalyst was well-mixed with the sugar solution, a sample was taken out to determine the initial sugar concentration as the reference. The vial was sealed with a PTFE/silicone septum and metal crimp top and placed in an oil bath located on a digital hot plate (Fisher Scientific). After the reaction was completed, the vial was placed in an ice bath for immediate cooling. A small amount of sample was extracted using a syringe and filtered through a 0.2 μm microfilter (Sigma-Aldrich) into a small vial. Then 200 μL of the filtered sample and 1 mL of an 8 mg/mL D-mannitol (Alfa, 99%) aqueous solution (used as an internal standard) were mixed in a high-performance liquid chromatography (HPLC) vial. The composition of the samples was determined on a PerkinElmer HPLC system equipped with an evaporative light scattering detector (Alltech 3000) and a photodiode array ultraviolet detector (PerkinElmer). A Bio-Rad Aminex HPX-87C column operated at 60 °C with HPLC-grade water as the mobile phase at a flow rate of 0.6 mL/min was employed to separate the reaction products.

3. RESULTS AND DISCUSSION

3.1. Studies of the Activity and Selectivity of Molybdenum-Based POMs toward Aldose Epimerization. The aldose conversion and selectivity data resulting from the reactions catalyzed by molybdenum-based POM catalysts are shown in Table 1. Entries 2, 4, 5, and 6 of Table 1 show that all of the molybdenum-based POM catalysts ($H_3PMo_{12}O_{40}$, $Ag_3PMo_{12}O_{40}$, and $Sn_{0.75}PMo_{12}O_{40}$) resulted in near-equilibrium glucose conversions[41] and high mannose selectivities (>90%) within 60 min of operation at 80 and 100 °C, independent of the nature of the cation in the structure (H^+, Ag^+, Sn^{4+}). For all of the runs, no significant side products were detected using HPLC. These results suggest that the cation does not participate in activating the reaction. In addition, the high activities and selectivities of the molybdenum-based POMs toward glucose epimerization were maintained as the pH was varied using HCl and NH_4OH, as shown in entries 1 and 3 of Table 1 and in Tables S1−S3 in the Supporting Information. We also found that replacing Mo with W in the Keggin structure POM resulted in loss of the activity (Table 1, entry 10), indicating that the molybdenum octahedra located in the cagelike structure of the POM play an important role in activating the epimerization of glucose.

We showed that the activity of molybdenum-based POMs toward the epimerization is not limited to glucose but extends to other aldoses such as xylose, as shown in entry 9 of Table 1. In addition, the Keggin anion was easily recovered and recycled from the reaction medium via precipitation using Ag^+ or Sn^{4+} ions. Entries 11−13 of Table 1 show the conversions and selectivities of the recycled POM for different recycle experiments. The recycled catalysts in all of the runs exhibited activities similar to that of the original catalyst, suggesting that no irreversible decomposition of the catalyst occurred under the reaction conditions.

The importance of surface molybdenum-based octahedra in Keggin structure molybdenum-based POMs in catalyzing the epimerization of glucose was further supported by the observation that the conversion of glucose increased with an increase in the concentration of Mo atoms. Figure 1 shows a plot of our reaction data where the molar ratio of Mo to glucose was varied to investigate the effect of the Mo concentration on the reaction rate within 60 min of operation at 80 °C. Figure 1 shows that the glucose conversion increased with an increase in the molar ratio of Mo to glucose up to a molar ratio of 1:50, at which point the glucose concentration started becoming the limiting factor. On the other hand, the

dx.doi.org/10.1021/cs401253z | ACS Catal. 2014, 4, 1358−1364

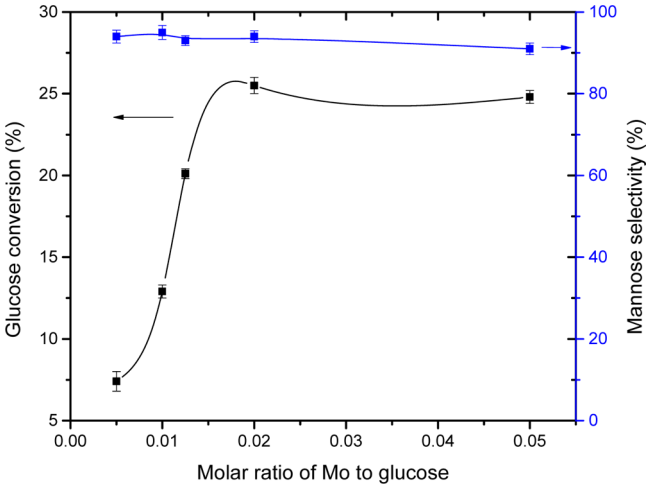

Figure 1. Correlation between glucose conversion and the molar ratio of Mo to glucose for glucose epimerization catalyzed by $H_3PMo_{12}O_{40}$ at 80 °C for 60 min of operation.

mannose selectivity remained unchanged, as expected since the nature of the active site did not change.

In addition to epimerizing glucose to mannose, molybdenum-based POMs are also highly active and selective in catalyzing the reverse reaction (Table 1, entries 7 and 8). However, under the same conditions, the reaction rate for glucose epimerization was higher than that for mannose epimerization. Figure 2 shows plots of the ratio of the

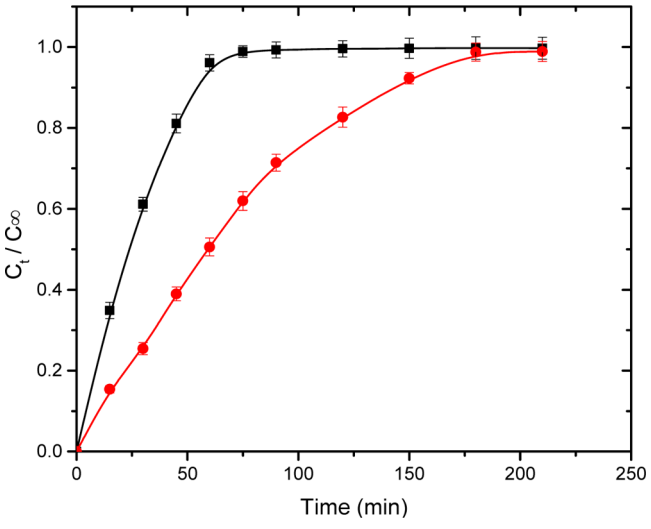

Figure 2. Plots of the ratio of the concentration of the product epimer at each time point (C_t) to its equilibrium concentration (C_∞) vs time: (black ■) glucose → mannose; (red ●) mannose → glucose. The reactions were run at 80 °C, and the molar ratio of Mo to glucose (or mannose) was kept constant at 1:50.

concentration of the product epimer to its equilibrium concentration as a function of time when $H_3PMo_{12}O_{40}$ was used as the catalyst. The equilibrium concentrations were calculated on the basis of previous reports.[41] It is clear from Figure 2 that glucose reaches equilibrium at a shorter time than mannose. This difference between the reaction rates for glucose and mannose epimerization is potentially due to the difference in the binding of the reactant molecules (glucose and mannose) to the active site, the Mo octahedra on the surface of $H_3PMo_{12}O_{40}$. Literature reports have shown that the binding of mannose to dimolybdate complexes results in less reactive species compared with glucose.[1] Because of the similar nature of Mo in these systems, a similar mechanism could govern the difference in the activities of glucose and mannose epimerization on molybdenum-based POMs. Further in situ NMR studies are necessary to support this hypothesis.

3.2. Characterization of the Catalytic System. A series of ^{31}P NMR studies were performed before and after the reaction to detect any decomposition of the molybdenum-based POM during the reaction. The ^{31}P NMR spectrum of the 0.1 M solution of $H_3PMo_{12}O_{40}$ without glucose (Figure 3a)

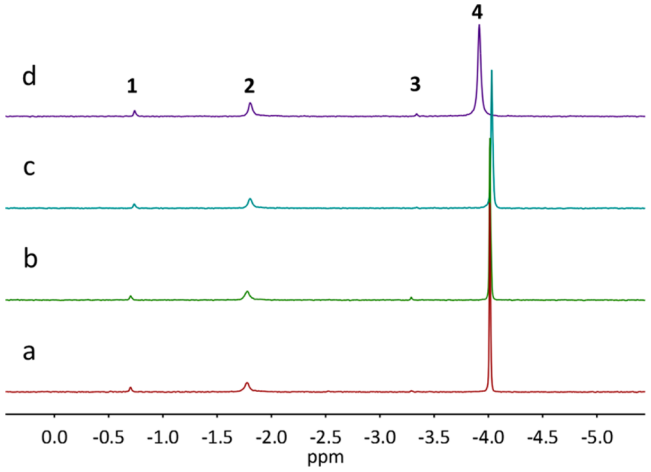

Figure 3. $^{31}P\{^1H\}$ spectra of a 0.1 M $H_3PMo_{12}O_{40}$ solution (a, c) before and (b, d) after heating at 80 °C for 60 min in (a, b) the absence and (c, d) the presence of glucose.

shows four expected P species in solution, in good agreement with the literature reports.[33,34] ^{31}P DOSY NMR studies were used to compare the molecular weights of these species on the basis of their diffusion rates (species 1, 2 > species 4 > species 3; Figure S1 in the Supporting Information).

On the basis of literature reports and our ^{31}P DOSY NMR results, species 4 was identified as $PMo_{12}O_{40}^{3-}$, species 3 as $P_2Mo_{18}O_{62}^{6-}$, and species 1 and 2 as derivatives of $PMo_{12}O_{40}^{3-}$ and $P_2Mo_{18}O_{62}^{6-}$ known as lacunary Keggin structures.[42−44] ^{31}P NMR studies of $H_3PMo_{12}O_{40}$ in aqueous solution after heating at 80 °C for 60 min showed no changes in the ^{31}P NMR spectrum of $H_3PMo_{12}O_{40}$ (Figure 3a,b), indicating that heating the catalyst in water to the reaction temperature resulted in no decomposition of the catalyst. When glucose was added to the 0.1 M $H_3PMo_{12}O_{40}$ solution and reaction occurred, the fourth peak, corresponding to $PMo_{12}O_{40}^{3-}$, exhibited a chemical shift accompanied by line broadening (Figure 3c,d and Table S5 in the Supporting Information). Literature reports have shown that the chemical shift and line broadening of $PMo_{12}O_{40}^{3-}$ are associated with the formation of the reduced form of $PMo_{12}O_{40}^{3-}$ (also known as heteropoly blue), which is in equilibrium with the oxidized parent (see eq 1); this equilibrium leads to the line broadening of the peak.[45,46] On the basis of these insights, our studies suggest that upon interaction with glucose, $PMo_{12}O_{40}^{3-}$ withdraws electrons from glucose, changing the oxidation state of Mo from +6 to +5 and establishing the following equilibrium:[45]

$$PMo^{VI}{}_{12}O_{40}^{3-} + ne^- \rightleftarrows PMo^{V}{}_{n}Mo^{VI}{}_{(12-n)}O_{40}^{(3+n)-} \quad (1)$$

dx.doi.org/10.1021/cs401253z | ACS Catal. 2014, 4, 1358−1364

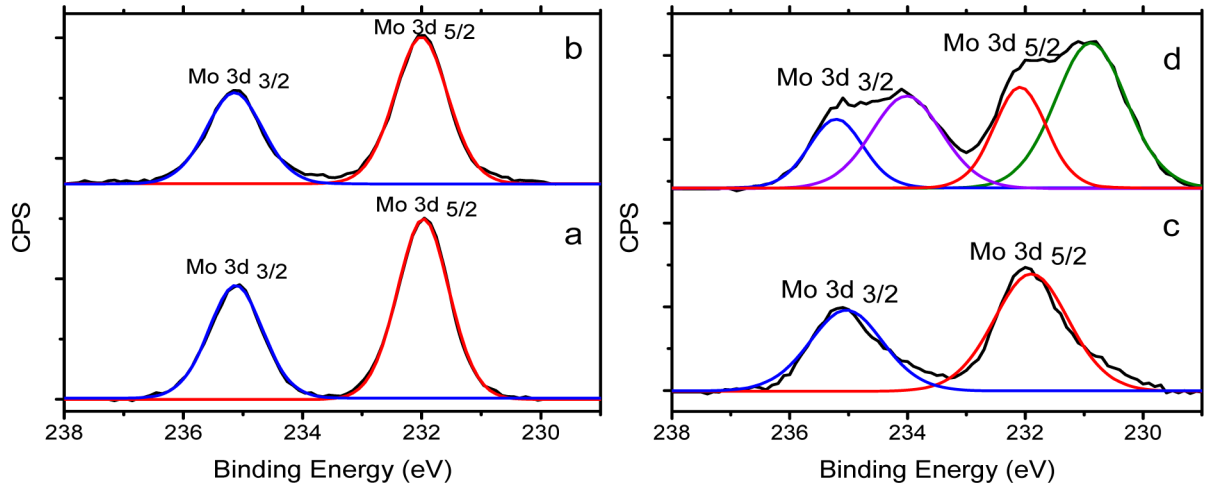

Figure 4. XPS spectra of Mo in $Ag_3PMo_{12}O_{40}$ obtained from precipitation of $PMo_{12}O_{40}^{3-}$ from solution using $AgNO_3$ (a, c) before and (b, d) after heating at 80 °C for 60 min in (a, b) the absence and (c, d) the presence of glucose. Black lines represent experimental data, blue lines represent fits for Mo $3d_{3/2}$ of Mo^{6+}, red lines represent fits for Mo $3d_{5/2}$ of Mo^{6+}, the violet line represents the fit for Mo $3d_{3/2}$ of Mo^{5+}, and the green line represents the fit for Mo $3d_{5/2}$ of Mo^{5+}.

The change in the oxidation state of Mo was also verified by XPS experiments (Figure 4). Figure 4a,b shows the XPS spectra for Mo in $Ag_3PMo_{12}O_{40}$ extracted before and after the catalyst was heated in water at 80 °C for 60 min without glucose. No changes in the spectrum were observed after heating. However, the Mo XPS spectrum of the $PMo_{12}O_{40}^{3-}$ extracted using $AgNO_3$ after the reaction with glucose shows the presence of Mo^{5+} states, as corroborated by the presence of the Mo $3d_{5/2}$ (230.9 eV) and $3d_{3/2}$ (234.0 eV) peaks at lower binding energies than the original states (232.0 and 235.1 eV, respectively) (Figure 4c,d). This suggests that the oxidation state of some of the Mo atoms was reduced from +6 to +5. These results are in good agreement with our ^{31}P NMR experiments discussed above supporting the formation of the reduced form of POM due to the electron donation from glucose. Similar results were obtained when $SnCl_4$ was used to extract $PMo_{12}O_{40}^{3-}$ from the reaction solution (Figure S3 in the Supporting Information). This unique electron transfer from glucose to the POM could play a significant role in activating the epimerization of glucose to mannose and is the objective of our future studies.

FTIR and XRD studies (Figures S4 and S5, respectively, in the Supporting Information) were used to characterize the morphology of the catalyst before and after reaction. Figure S5 shows the XRD patterns for $Ag_3PMo_{12}O_{40}$ (a) before and (b) after heating to 80 °C for 60 min and (c) before and (d) after reaction with glucose at 80 °C for 60 min. No detectable changes in the XRD patterns were observed under any of these conditions, again emphasizing the fact that the Keggin structure of the molybdenum-based POMs is preserved after the epimerization of glucose. Similar results were obtained from the FTIR studies shown in Figure S4.

In summary, the characterizations of the catalysts before and after reaction suggest that (i) no decomposition of the molybdenum-based POMs occurs under the reaction conditions and (ii) electron transfer occurs upon the interaction of the molybdenum-based POM with glucose, leading to a change in the oxidation state of Mo atoms and the formation of the reduced form of the POM (heteropoly blue). The effect of the electron transfer that leads to the formation of the heteropoly blue on the catalytic cycle is of great interest and still under investigation.

3.3. Kinetic Study of Glucose Epimerization with $H_3PMo_{12}O_{40}$, $Ag_3PMo_{12}O_{40}$, and $Sn_{0.75}PMo_{12}O_{40}$. Controlled kinetic experiments were conducted to determine the apparent activation barriers for glucose epimerization using molybdenum-based POMs. Figure 5 shows the initial turnover rates for glucose epimerization using $H_3PMo_{12}O_{40}$, $Ag_3PMo_{12}O_{40}$, and $Sn_{0.75}PMo_{12}O_{40}$ as functions of temperature. The initial turnover rates (per mole of Mo) of glucose epimerization measured over $H_3PMo_{12}O_{40}$, $Ag_3PMo_{12}O_{40}$ and $Sn_{0.75}PMo_{12}O_{40}$ depend similarly on temperature over the range of 343−393 K. These results again reinforce the fact that the active sites responsible for glucose epimerization in the catalytic systems ($H_3PMo_{12}O_{40}$, $Ag_3PMo_{12}O_{40}$, and $Sn_{0.75}PMo_{12}O_{40}$) are the surface Mo octahedra, independent of the countercation (H^+, Ag^+, or Sn^{4+}). The turnover rates were calculated on the basis of the assumption that the glucose

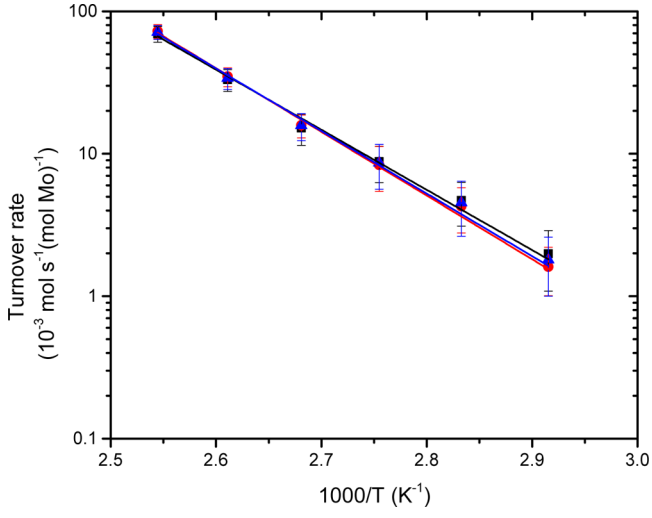

Figure 5. Temperature dependence of the initial turnover rates over $H_3PMo_{12}O_{40}$ (black line), $Sn_{0.75}PMo_{12}O_{40}$ (blue line), and $Ag_3PMo_{12}O_{40}$ (red line) for glucose epimerization to mannose.

dx.doi.org/10.1021/cs401253z | ACS Catal. 2014, 4, 1358−1364

epimerization catalyzed by $H_3PMo_{12}O_{40}$, $Ag_3PMo_{12}O_{40}$, or $Sn_{0.75}PMo_{12}O_{40}$ is a first-order reaction. The initial (t = 0 min) turnover rates (per mole of Mo) for glucose epimerization to mannose were determined from extrapolation to t = 0 min. The apparent activation energies were calculated to be 96 ± 4, 99 ± 4, and 97 ± 3 kJ/mol for $H_3PMo_{12}O_{40}$, $Ag_3PMo_{12}O_{40}$, and $Sn_{0.75}PMo_{12}O_{40}$, respectively, on the basis of the slopes of the plots in Figure 5. These apparent activation barriers are much lower than the one reported for glucose epimerization using molybdate catalysts under acidic conditions (~126 kJ/mol).[47]

3.4. Isotope-Labeling Experiments To Elucidate the Mechanism of Glucose Epimerization. In order to determine the mechanism involved in the epimerization of aldoses, we conducted ^{13}C NMR experiments with isotopically labeled [^{13}C1]glucose (i.e., C1 in glucose labeled with ^{13}C). The ^{13}C NMR spectra of unlabeled glucose in aqueous solution with $H_3PMo_{12}O_{40}$ before and after reaction are shown in Figure 6c,d, respectively. All of the positional assignments for each carbon atom in α- and β-D-glucose and -mannose are shown according to literature reports.[48]

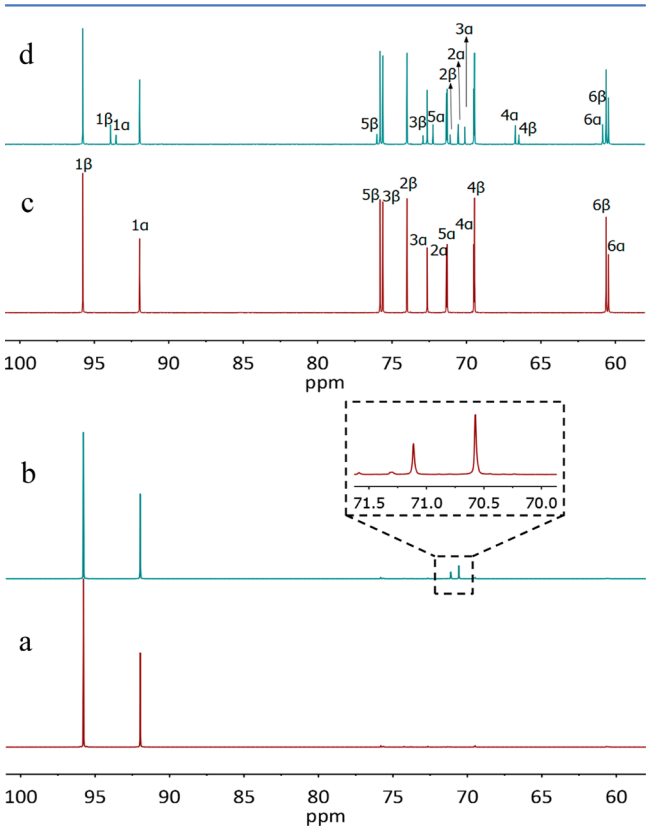

Figure 6. $^{13}C\{^1H\}$ NMR spectra of (a, b) glucose labeled at the C1 position and (c, d) unlabeled glucose in aqueous solution with $H_3PMo_{12}O_{40}$ (a, c) before and (b, d) after reaction at 80 °C for 60 min.

The new signals appearing after reaction indicate the formation of mannose, which was also confirmed by HPLC. In the case of the experiments with isotopically labeled [^{13}C1]glucose, the signal for C1 is much more intense than for the other carbons (the signal intensities of the other carbons are negligible compared with that of the enriched C1). Figure 6a shows the ^{13}C NMR spectrum before reaction of a 10% (w/w) [^{13}C1]glucose solution containing $H_3PMo_{12}O_{40}$ in a 1:50 Mo:glucose molar ratio before reaction, with signals at 95.8 and 92.0 ppm. These signals correspond to C1 of the β and α configurations of [^{13}C1]glucose. After reaction (Figure 6b), a new set of signals appear at 71.1 and 70.6 ppm, which correspond to the chemical shifts of C2 of the β and α forms of [^{13}C2]mannose.[48] These results demonstrate that a C1−C2 intramolecular carbon exchange occurs during the epimerization of glucose to mannose using molybdenum-based POM catalysts.

To further support the intramolecular C1−C2 shift during the epimerization of glucose, ^{13}C kinetic isotope effect studies on the reaction rate were conducted. Once again C1 in glucose was labeled with ^{13}C, and the reaction rates were measured and compared with the case of unlabeled glucose at 353 K. Figure 7 shows the mannose concentrations as functions of time for the reactions with [^{13}C1]glucose and unlabeled glucose. The rate constant at 353 K for epimerization of unlabeled glucose is higher than that for the glucose labeled at C1 by a factor of 1.06 ± 0.03. This is similar to the kinetic isotope effect calculated using transition-state theory assuming that the intramolecular C1−C2 shift is the rate-limiting step (details can be found in section S.4 in the Supporting Information).[49]

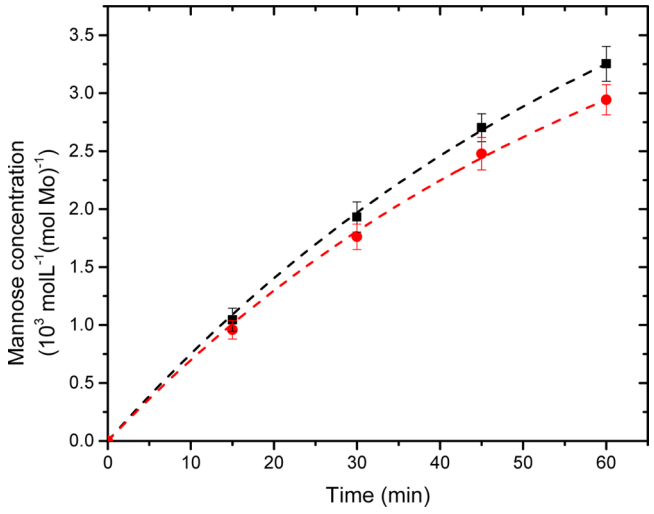

Figure 7. Concentration of mannose as a function of reaction time during the reaction of a 10% (w/w) solution of glucose (black ■) and glucose labeled with ^{13}C at C1 (red ●) using $H_3PMo_{12}O_{40}$ as the catalyst at 80 °C. Dashed curves are fits of the experimental data assuming that glucose epimerization is a first-order reaction. Initial (t = 0 min) turnover rates (per mole of Mo) for glucose epimerization to mannose were determined from extrapolation to t = 0 min (details can be found in section S.3 in the Supporting Information).

4. CONCLUSION

We have demonstrated for the first time that molybdenum-based POMs are active and selective catalysts for the epimerization of aldoses. The process of epimerization of aldoses using molybdenum-based POMs ($H_3PMo_{12}O_{40}$, $Ag_3PMo_{12}O_{40}$, and $Sn_{0.75}PMo_{12}O_{40}$) as catalysts involves electron transfer from the aldose to the Mo octahedra surface units of the POM followed by an intramolecular C1−C2 carbon shift. The apparent activation barriers for glucose epimerization on $H_3PMo_{12}O_{40}$, $Ag_3PMo_{12}O_{40}$, and $Sn_{0.75}PMo_{12}O_{40}$ were determined to be 96 ± 4, 99 ± 4, and 97 ± 3 kJ/mol, respectively. These apparent activation barriers are significantly lower than the activation barrier reported for

dx.doi.org/10.1021/cs401253z | ACS Catal. 2014, 4, 1358−1364

the molybdate-based catalysts (i.e., molybdic acid). In addition, we have shown that Keggin structure molybdenum-based POMs are stable and do not decompose under the reaction conditions. The catalyst can be easily extracted from solution and recycled for a number of cycles. These findings pave the way for the implementation of Keggin structure molybdenum-based POMs as single, easy to separate, and recyclable catalytic systems for the epimerization of aldoses under aqueous conditions.

■ ASSOCIATED CONTENT

Supporting Information

Experimental and characterization details. This material is available free of charge via the Internet at http://pubs.acs.org.

■ AUTHOR INFORMATION

Corresponding Author

*E-mail: erandan@wayne.edu.

Notes

The authors declare no competing financial interest.

■ ACKNOWLEDGMENTS

We gratefully acknowledge the support of the National Science Foundation (CBET-1226569) and Wayne State University. We thank Dr. Kai Sun for his help with XPS and Prof. Mark Barteau for helpful discussions.

■ REFERENCES

(1) Hayes, M. L.; Pennings, N. J.; Serianni, A. S.; Barker, R. *J. Am. Chem. Soc.* **1982**, *104*, 6764−6769.
(2) Granstrom, T. B.; Takata, G.; Tokuda, M.; Izumori, K. *J. Biosci. Bioeng.* **2004**, *97*, 89−94.
(3) Gumina, G.; Song, G. Y.; Chu, C. K. *FEMS Microbiol. Lett.* **2001**, *202*, 9−15.
(4) Kamm, B. *Angew. Chem., Int. Ed.* **2007**, *46*, 5056−5058.
(5) Murata, A.; Sekiya, K.; Watanabe, Y.; Yamaguchi, F.; Hatano, N.; Izumori, K.; Tokuda, M. *J. Biosci. Bioeng.* **2003**, *96*, 89−91.
(6) Lu, Y.; Levin, G. V.; Donner, T. W. *Diabetes, Obes. Metab.* **2008**, *10*, 109−134.
(7) Bílik, V.; Biely, P.; Kolina, J. *Chem. Zvesti* **1984**, *38*, 491−498.
(8) Glaser, L. In *The Enzymes*; Boyer, P. D., Ed.; Academic Press: New York, 1972; Vol. *6*, pp 355−380.
(9) Nguyen, Q. A.; Saddler, J. N. *Bioresour. Technol.* **1991**, *35*, 275−282.
(10) Morgan, P. M.; Sala, R. F.; Tanner, M. E. *J. Am. Chem. Soc.* **1997**, *119*, 10269−10277.
(11) Angyal, S. J.; Craig, D. C. *Carbohydr. Res.* **1993**, *241*, 1−8.
(12) El Khadem, H. S.; Ennifar, S.; Isbell, H. S. *Carbohydr. Res.* **1987**, *169*, 13−21.
(13) Yang, B. Y.; Montgomery, R. *Carbohydr. Res.* **1996**, *280*, 27−45.
(14) Bílik, V. *Chem. Zvesti* **1972**, *26*, 183−186.
(15) Bílik, V. *Chem. Zvesti* **1972**, *26*, 372−375.
(16) Bílik, V.; Stankovič, L. *Chem. Zvesti* **1973**, *27*, 544−546.
(17) Tanase, T.; Shimizu, F.; Kuse, M.; Yano, S.; Hidai, M.; Yoshikawa, S. *Inorg. Chem.* **1988**, *27*, 4085−4094.
(18) Takizawa, S.; Sugita, H.; Yano, S.; Yoshikawa, S. *J. Am. Chem. Soc.* **1980**, *102*, 7969−7971.
(19) Tanase, T.; Shimizu, F.; Yano, S.; Yoshikawa, S. *J. Chem. Soc., Chem. Commun.* **1986**, 1001−1003.
(20) Osanai, S.; Inaba, K.; Yoshikawa, S. *Carbohydr. Res.* **1991**, *209*, 289−295.
(21) Yamauchi, T.; Fukushima, K.; Yanagihara, R.; Osanai, S.; Yoshikawa, S. *Carbohydr. Res.* **1990**, *204*, 233−239.
(22) Asperger, R. G.; Liu, C. F. *Inorg. Chem.* **1965**, *4*, 1395−1397.
(23) Bermejo-Deval, R.; Gounder, R.; Davis, M. E. *ACS Catal.* **2012**, *2*, 2705−2713.
(24) Gunther, W. R.; Wang, Y. R.; Ji, Y. W.; Michaelis, V. K.; Hunt, S. T.; Griffin, R. G.; Roman-Leshkov, Y. *Nat. Commun.* **2012**, *3*, 1109−1116.
(25) Pope, M. T. *Heteropoly and Isopoly Oxometalates*; Springer: Berlin, 1983.
(26) Nakagawa, Y.; Kamata, K.; Kotani, M.; Yamaguchi, K.; Mizuno, N. *Angew. Chem., Int. Ed.* **2005**, *44*, 5136−5141.
(27) Clemente-Juan, J. M.; Coronado, E. *Coord. Chem. Rev.* **1999**, *193*−*195*, 361−394.
(28) Kögerler, P.; Tsukerblat, B.; Müller, A. *Dalton Trans.* **2010**, *39*, 21−36.
(29) Hasenknopf, B. *Front. Biosci.* **2005**, *10*, 275−287.
(30) Hill, C. L. *J. Mol. Catal. A: Chem.* **2007**, *262*, 1.
(31) He, T.; Yao, J. N. *Prog. Polym. Sci.* **2006**, *51*, 810−879.
(32) Kozhevnikov, I. V. *Catal. Rev.: Sci. Eng.* **1995**, *37*, 311−352.
(33) Zhang, J. Z.; Liu, X.; Hedhili, M. N.; Zhu, Y. H.; Han, Y. *ChemCatChem* **2011**, *3*, 1294−1298.
(34) Ntainjua, E. N.; Piccinini, M.; Freakley, S. J.; Pritchard, J. C.; Edwards, J. K.; Carley, A. F.; Hutchings, G. J. *Green Chem.* **2012**, *14*, 170−181.
(35) Wolfel, R.; Taccardi, N.; Bosmann, A.; Wasserscheid, P. *Green Chem.* **2011**, *13*, 2759−2763.
(36) Kanno, M.; Yasukawa, T.; Ninomiya, W.; Ooyachi, K.; Kamiya, Y. *J. Catal.* **2010**, *273*, 1−8.
(37) Chuvaev, V. F.; Popov, K. I.; Spitsyn, V. I. *Dokl. Akad. Nauk SSSR* **1980**, *255*, 892−895.
(38) Izumi, Y.; Hasebe, R.; Urabe, K. *J. Catal.* **1983**, *84*, 402−409.
(39) Ghanbari-Siahkali, A.; Philippou, A.; Dwyer, J.; Anderson, M. W. *Appl. Catal., A* **2000**, *192*, 57−69.
(40) Shimizu, K.-i.; Niimi, K.; Satsuma, A. *Appl. Catal., A* **2008**, *349*, 1−5.
(41) Angyal, S. J. *Angew. Chem., Int. Ed. Engl.* **1969**, *8*, 157−166.
(42) Massart, R.; Contant, R.; Fruchart, J. M.; Ciabrini, J. P.; Fournier, M. *Inorg. Chem.* **1977**, *16*, 2916−2921.
(43) Pettersson, L.; Andersson, I.; Ohman, L. O. *Inorg. Chem.* **1986**, *25*, 4726−4733.
(44) Davison, S. F.; Mann, B. E.; Maitlis, P. M. *J. Chem. Soc., Dalton Trans.* **1984**, 1223−1228.
(45) Greenwood, N. N.; Earnshaw, A. *Chemistry of the Elements*, 2nd ed.; Butterworth-Heinemann: Oxford, U.K., 1997.
(46) Kozik, M.; Hammer, C. F.; Baker, L. C. W. *J. Am. Chem. Soc.* **1986**, *108*, 7627−7630.
(47) Cybulski, A.; Kuster, B. F. M.; Marin, G. B. *J. Mol. Catal.* **1991**, *68*, 87−103.
(48) Kingmorris, M. J.; Serianni, A. S. *J. Am. Chem. Soc.* **1987**, *109*, 3501−3508.
(49) Frantz, D. E.; Singleton, D. A.; Snyder, J. P. *J. Am. Chem. Soc.* **1997**, *119*, 3383−3384.